JACS
JOURNAL OF THE AMERICAN CHEMICAL SOCIETY
Article
pubs.acs.org/JACS

Bimolecular Photoinduced Electron Transfer Beyond the Diffusion Limit: The Rehm−Weller Experiment Revisited with Femtosecond Time Resolution

Arnulf Rosspeintner,[†] Gonzalo Angulo,[‡] and Eric Vauthey*[,†]

[†]Department of Physical Chemistry, University of Geneva, 30 Quai Ernest-Ansermet, 1211 Genève 4, Switzerland
[‡]Institute of Physical Chemistry, Polish Academy of Sciences, Kasprzaka 44/52, 01-224 Warsaw, Poland

Supporting Information

ABSTRACT: To access the intrinsic, diffusion free, rate constant of bimolecular photoinduced electron transfer reactions, fluorescence quenching experiments have been performed with 14 donor/acceptor pairs, covering a driving-force range going from 0.6 to 2.4 eV, using steady-state and femtosecond time-resolved emission, and applying a diffusion-reaction model that accounts for the static and transient stages of the quenching for the analysis. The intrinsic electron transfer rate constants are up to 2 orders of magnitude larger than the diffusion rate constant in acetonitrile. Above ∼1.5 eV, a slight decrease of the rate constant is observed, pointing to a much weaker Marcus inverted region than those reported for other types of electron transfer reactions, such as charge recombination. Despite this, the driving force dependence can be rationalized in terms of Marcus theory.

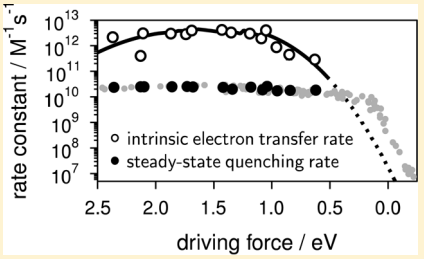

INTRODUCTION

Since its formulation in the mid-1950s,[1] Marcus theory of electron transfer (ET) reactions has been intensively put to the test, in particular, its prediction of a quadratic free-energy relationship contrasted with the linear free-energy relationships that were prevailing among chemists.[2−4] Oxidation/reduction reactions in the electronic ground state were quickly found to be well described using Marcus theory,[5,6] but their driving forces were not large enough to test the presence of the so-called Marcus inverted region (MIR), i.e. the decrease of the reaction rate with increasing driving force. However, larger driving forces can be achieved with photoinduced charge separation (CS) and, in the late 1960s, an experiment by Rehm and Weller cast serious doubt on the validity of Marcus theory for describing photoinduced electron transfer reactions.[7,8] Indeed, the rate constant of bimolecular photoinduced CS was found to increase with driving force up to a value that corresponds to that of the diffusion of the reactants, and to remain diffusion limited even at driving forces where inversion is expected. The MIR had to wait until the mid-1980s to be experimentally observed for intramolecular charge shift reactions.[9,10] Since then, it has been reported for many different types of ET processes: intramolecular charge recombination,[11] intermolecular charge recombination,[12−14] intermolecular charge shift,[15,16] intramolecular charge separation,[17] and charge separation in hydrogen-bonded complexes.[18]

However, so far there has been no convincing experimental observation of the MIR for bimolecular photoinduced CS reactions in liquid solution. We have recently shown that the observations of the MIR in restricted environments or high-viscous media are, in fact, spurious and due to a neglect of the static and transient stages of the ET quenching in the analysis.[19] The apparent discrepancy between experiment and theory, inherent to this specific type of reaction, has continuously attracted the attention of photochemists to the point that it has become quasi-textbook knowledge that the nonobservation of the MIR in the Rehm−Weller-type experiment is simply due to the masking of the intrinsic electron transfer dynamics by diffusion.[20] Nonetheless, over the years, several additional explanations for the lack of the MIR were proposed. Rehm and Weller, in their original paper, had already suggested that the absence of the MIR could arise from the existence of additional CS pathways leading to the ionic product in an electronic excited state.[8] The possibility for such a pathway to suppress the inverted region has been examined theoretically by Marcus.[21] We have recently obtained direct experimental evidence of such CS to an excited product for several donor/acceptor pairs, whose CS to the ground-state product is expected to be in the inverted regime.[22] On the other hand, Mataga and co-workers invoked dielectric saturation, i.e. the breakdown of the linear dielectric response approximation,[23] whereas Tachiya and Murata,[24] Burshtein and Ivanov,[25] as well as Rosspeintner et al.[26] proposed that the absence of the MIR could be rationalized by the distance dependence of the solvent reorganization energies, that favors remote CS as the driving force increases.[27]

Several groups attempted to extract the intrinsic ET rates from the analysis of the nonexponential decays of the excited chromophore population measured using ultrafast spectrosco-

Received: November 22, 2013
Published: January 8, 2014

   dx.doi.org/10.1021/ja4118279 | J. Am. Chem. Soc. 2014, 136, 2026−2032

py. Seminal works by the groups of Tachiya,[28] Fleming,[29] and Fayer[30] significantly contributed to our understanding of the non-Markovian nature of the dynamics of bimolecular CS, but were focused on a small number of donor/acceptor pairs, only covering a limited range of driving force. Mataga and co-workers,[31] as well as Angel and Peters,[32] on the other hand, investigated various systems, spanning a larger driving force range, but disregarded steady-state emission experiments as reference. The so-obtained intrinsic electron transfer rate constants exhibited relatively large scatter, rendering the observation of systematic trends impossible.

Here, we present a comprehensive investigation of the intrinsic photoinduced CS rate constant of 14 donor/acceptor pairs (Chart 1 and Table 1) in acetonitrile covering a driving force range from 0.63 to 2.37 eV, using steady-state and femtosecond time-resolved emission spectroscopies. The experimental data were analyzed with a diffusion-assisted reaction model using an extension of the semiclassical Marcus theory accounting for the finite dielectric response of the solvent. The combination of steady-state and femtosecond time-resolved emission spectroscopies and of a theory that properly accounts for diffusional effects, allowed the intrinsic electron transfer rate constant to be extracted and its free energy dependence to be determined. The so-obtained intrinsic CS rate constants show a distinct driving-force dependence with a very attenuated Marcus inversion at rates as high as 10^{12} M^{-1} s^{-1}, which can be satisfyingly rationalized within the framework of Marcus theory. This investigation, which can be considered as a femtosecond time-resolved analog of the original Rehm–Weller experiment, solves the long-standing apparent discrepancy between Marcus theory and the experimental results of Rehm and Weller.

Chart 1. (Top) Fluorophores (see Table 1 for the properties); (Bottom) Electron-Donating and -Accepting Quenchers with Their Respective Oxidation and Reduction Potentials (V vs SCE, from refs 8 and 33 for TMP)

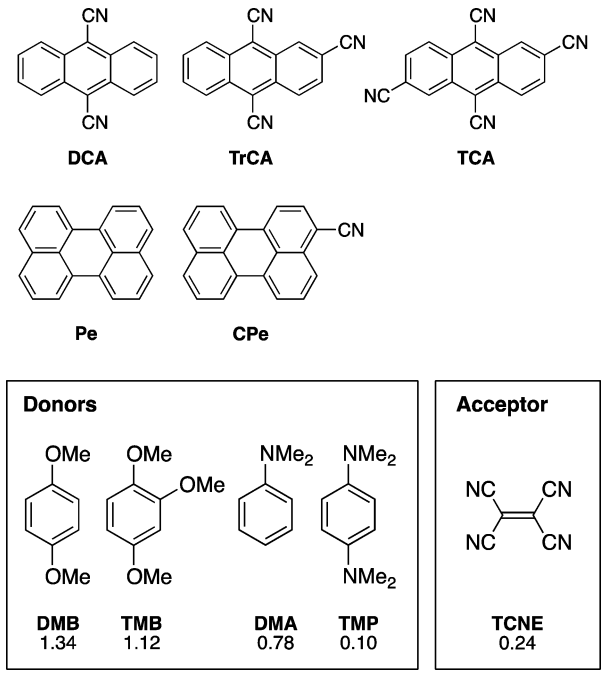

Table 1. Characteristic Electrochemical and Photophysical Properties of the Fluorophores in Acetonitrile at 20 °C

F	E (A/A^-) (V vs SCE)	E (D^+/D) (V vs SCE)	E_{00} [a] (eV)	τ_0 [b] (ns)
DCA	−0.98[c]	1.89[f]	2.89	14.6
TrCA	−0.70[d]	2.07[f]	2.85	18.4
TCA	−0.45[e]	2.20[f]	2.86	16.7
Pe	−1.76	1.00	2.83	5.5
CPe	−1.37	1.21	2.65	5.7

[a] S_1 state energy. [b] Fluorescence lifetime. [c] From ref 34. [d] From ref 35. [e] From ref 36. [f] From ref 37.

PRINCIPLE OF THE EXPERIMENT

The mechanism of the photoinduced CS investigated here is represented in Scheme 1. The occurrence of CS is confirmed by previous ultrafast spectroscopy measurements that show the formation of the ionic products.[38−40] The equilibrium constant K_{CT} accounts for the possible formation of ground-state complex between fluorophore (F) and quencher (Q).

Scheme 1. Bimolecular Charge Separation between an Excited Fluorophore (F) and a Quencher (Q)

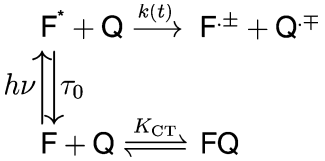

Because the distribution of distances between the fluorophore and the quenchers evolves with time just after excitation, the quenching rate coefficient, $k(t)$, is time-dependent, as illustrated in Figure 1.[19,41,42] Directly after excitation, CS takes place between reactants that are already at optimal distances and, as no diffusion is needed, the quenching is entirely static and proceeds with the intrinsic rate constant of the elementary process, k_0. At later times, the reaction becomes more and more diffusion controlled, with $k(t)$ slowing down until the rates of mutual approach of the reactants via diffusion and their disappearance upon CS have equilibrated at k_∞. Consequently, the experimentally observable decay of the fluorescence intensity, $I(t,c)$, is nonexponential and is given by:[41−43]

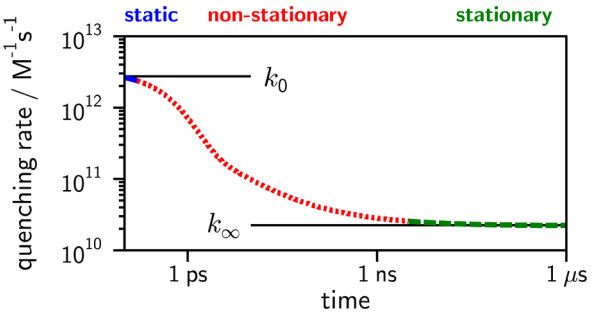

Figure 1. Time dependence of the reaction rate coefficient, $k(t)$, of a diffusion-assisted bimolecular electron transfer reaction. The reaction rate coefficient changes from the static or intrinsic rate of electron transfer, k_0, until reaching the stationary, i.e. diffusional, rate constant, k_∞.

dx.doi.org/10.1021/ja4118279 | J. Am. Chem. Soc. 2014, 136, 2026−2032

$$I(t, c) = \exp\left(-\frac{t}{\tau_0} - c\int_0^t k(t')\,dt'\right) = I(t, 0)\exp\left(-c\int_0^t k(t')\,dt'\right) \quad (1)$$

where c is the quencher concentration and τ_0 the fluorescence lifetime at $c = 0$.

On the other hand, the steady-state quenching rate coefficient, κ, is concentration dependent. In particular, $\kappa(c)$ increases with the quencher concentration, as the overall reaction becomes more and more dominated by the static and transient stages of the quenching. This quantity can be obtained from the decrease of the steady-state fluorescence intensity, ϕ, upon addition of Q:[41−43]

$$\frac{\phi(0)}{\phi(c)}\cdot\frac{1}{1 + cK_{CT}} = \frac{\int_0^\infty I(t, 0)\,dt}{\int_0^\infty I(t, c)\,dt} = 1 + \kappa(c)\tau_0 c \quad (2)$$

Figure 1 indicates that the stationary quenching rate constant, k_∞, can be obtained from the slowest decay component of the fluorescence, τ_{long}:

$$\frac{\tau_0}{\tau_{long}(c)} = 1 + k_\infty\tau_0 c \quad (3)$$

In principle, the intrinsic CS rate constant, k_0, can be accessed from the static stage of the quenching, i.e. from the analysis of the early fluorescence decay (Figure 1). As the relative contribution of static quenching increases with c, the extraction of k_0 is, in principle, easier at larger quencher concentrations. However, the validity of eq 1 should first be checked by ensuring that $k(t)$ itself does not depend on concentration. Steady-state quenching experiments are also useful, because $\kappa(c)$ in eq 2 reflects the integral of the whole fluorescence decay, and thus depends on k_0. Therefore, ultrafast decay components that might be missed in the time-resolved measurements, because of an insufficient time resolution, are seen in a steady-state quenching experiment. Whereas large concentrations favor the determination of k_0 from the fluorescence decay, they increase the error on $\kappa(c)$ obtained from the steady-state measurements as the observed integrated emission intensity becomes smaller. Because of these two adverse indications on the optimal concentration, combined steady-state and time-resolved emission experiments have been performed with overlapping concentration ranges.

RESULTS AND DISCUSSION

The ET quenching of 14 F/Q pairs (Chart 1) in acetonitrile has been measured using steady-state as well as femtosecond and nanosecond time-resolved fluorescence spectroscopy, namely fluorescence up-conversion and time-correlated single photon counting, respectively. Figures 2 and 3a illustrate the decrease of the steady-state emission intensity and the acceleration of the fluorescence decay of TrCA upon increasing DMA concentration. Both nanosecond and femtosecond time-resolved measurements showed nonexponential emission intensity decays, this feature being more pronounced in the femtosecond experiments (Figure 3a), where the static stage of the quenching can be resolved. In addition, for various F/Q pairs, a new, broad, unstructured and red-shifted absorption band was observed (Figure S1, Supporting Information [SI]). It can be attributed to a charge-transfer band from a ground-state

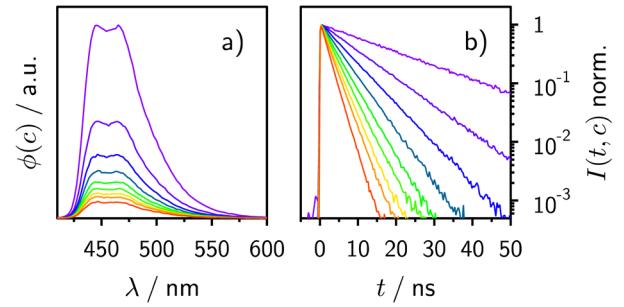

Figure 2. Effect of the addition of DMA (up to 0.02 M) on (a) the steady-state fluorescence intensity and (b) the nanosecond time-resolved fluorescence of TrCA.

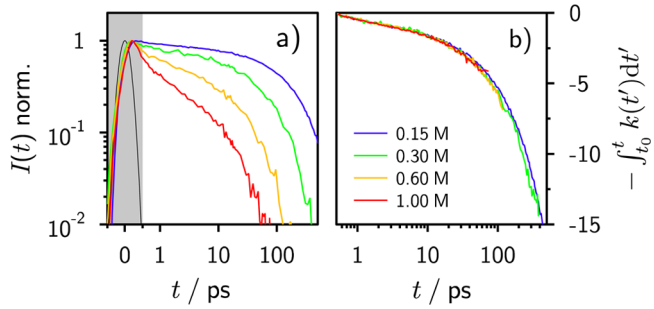

Figure 3. (a) Femtosecond-resolved time profiles of the fluorescence intensity measured with the TrCA/DMA pair (the black line is the instrument response function) and (b) after concentration normalization of the kinetics in the white area of part a) (see text).

complex.[39,44] However, the band shape of the emission spectra upon addition of quencher remained unchanged and no additional band could be observed, indicating that the excited complex does not emit, at least with the wavelength used to excite the fluorophores.

Figure 4 depicts the result of a Stern−Volmer experiment with the same F/Q pair in two representations. The

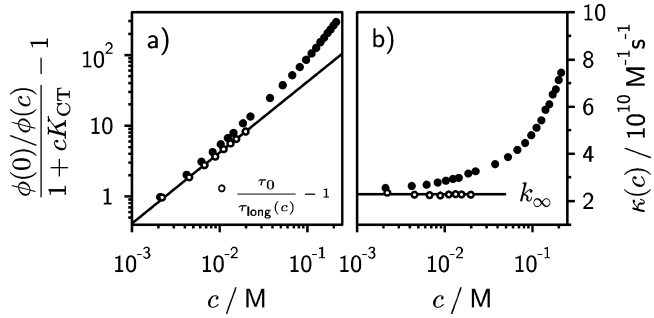

Figure 4. (a) Stern−Volmer representation of the quenching of TrCA by DMA determined from the steady-state fluorescence intensity (black) and the slowest fluorescence decay component, τ_{long}, (open circles). (b) Concentration dependence of κ(c) (black) and k_∞ (open), as defined in eqs 2 and 3

conventional Stern−Volmer plot (Figure 4a) constructed using the slowest decay component of the fluorescence, τ_{long}, is linear, as expected from eq 3, and the stationary quenching rate constant, k_∞, can be directly extracted from the slope. On the other hand, the plot made from the steady-state fluorescence intensity, ϕ, departs from linearity already at quencher concentrations above ~10^{-2} M, pointing to a

dx.doi.org/10.1021/ja4118279 | J. Am. Chem. Soc. 2014, 136, 2026−2032

concentration dependence of the quenching rate coefficient, κ. This is better seen in Figure 4b, which represents k_∞ and κ as a function of quencher concentration. This plot directly shows that indeed κ is concentration dependent, whereas k_∞ is not. Moreover, one can see that κ approaches k_∞ only at very low concentrations. In other words, even in a low viscosity solvent like acetonitrile, the quenching rate constants of diffusion-influenced reactions obtained from time-resolved and steady-state experiments are only similar when the quencher concentration tends to zero.

To ensure that the fluorescence time profiles can be properly analyzed using eq 1, namely that the time dependent quenching rate, $k(t)$, does not depend on concentration, they can be concentration-normalized to directly reflect the intrinsic reaction dynamics given by $\int_0^t k(t')\,dt'$. This was done by replacing the lower limit of the integral by a finite value, t_0, chosen to eliminate problems related to the convolution with the instrument response function, at the price of losing information about faster dynamics. The result of this normalization, performed with TrCA/DMA with t_0 = 0.5 ps, is illustrated in Figure 3b. A similar concentration independence of the reaction dynamics was found for all F/Q pairs investigated (Figure S4, SI).

The femtosecond time-resolved fluorescence decays measured at c = 0.15 M with all 14 F/Q pairs are compared in Figure S5, SI. Their overall aspect does not differ very much, especially when considering time delays above ~10 ps. However, a closer look at the first few picoseconds allows differences to be seen in the initial intensity decay. An acceleration of the rate can be clearly discerned when going from the lowest driving force, i.e. 0.63 eV, up to about 1.8 eV. At higher driving forces, this initial decay seems to rather slow down, although this effect is not very pronounced. A qualitatively similar trend exists for the steady-state quenching rate, $\kappa(c)$, at high concentrations. With the exception of Pe/TMP, κ(c) increases continuously with driving force up to about 1.8 eV, and decreases slightly with further increase of the exergonicity. These two qualitative comparisons point to a bell-shaped like free-energy dependence of the quenching rate constant in the static regime. However, really conclusive statements on the free-energy dependence of k_0 require a careful analysis of the time-resolved and steady-state data.

Extraction of k_0 directly from the experimental fluorescence decays by either direct differentiation of the concentration-normalized time-profiles as depicted in Figure 3b or using multiexponential analysis proved to be unsuccessful (cf. SI). Whereas the former approach requires an unrealistically high signal-to-noise ratio of the data, the multiexponential approach is simply an inadequate model for a diffusion-controlled process, the kinetics of which is intrinsically nonexponential.[41,45] As a consequence, a model that properly describes a diffusion-controlled ET reaction was used. To this end, a diffusion-reaction equation approach, namely differential encounter theory (DET), with a modified Marcus ET model was applied.[41,46−49] In the following, only the expression used for the ET probability, $w(r)$, i.e. the sink term in the diffusion-reaction equation, will be discussed, whereas the details of the diffusive part of the problem, being the same as in references 50 and 51 can be found in the SI.

For the ET rate, the expression obtained from non-perturbative semiclassical transition state theory, modified by Gould and co-workers,[52] was applied. This expression accounts for the population of vibrationally excited product states and the finite dielectric response of the environment using the appropriate Landau−Zener factors for ET in the normal and inverted regions. The difference in the Landau−Zener factors reflects the change of the nature of the ET process in the normal and inverted regions.[53] Here, the full expression with the coupling matrix element V in the exponent, which is valid even for large V is used:[54]

$$w(r) = \sum_n \frac{1}{\tau_s} A_n \exp\left(-\frac{(\Delta G(r) + n\hbar\omega + \lambda_s(r))^2}{4k_B T\lambda_s(r)}\right) \tag{4}$$

$$A_n = \begin{cases} \dfrac{(1-B_n)}{(2-B_n)} & \text{normal region, i.e. } \Delta G + n\hbar\omega + \lambda_s > 0 \\ (1-B_n)B_n & \text{inverted region, i.e. } \Delta G + n\hbar\omega + \lambda_s < 0 \end{cases}$$

$$B_n = \exp(-\tau_S U(r)\, e^{-S} S^n/n!) \tag{5}$$

where $U(r)$ is defined as

$$U(r) = V^2\, e^{-2(r-\sigma)/L} \sqrt{\frac{\pi}{\hbar^2 k_B T \lambda_s(r)}} \tag{6}$$

with $S = \lambda_{qm}/\hbar\omega$, λ_{qm} and ω denoting the reorganization energy and frequency of the quantum mode, respectively. L is the decay length of the coupling matrix element V and σ is the contact distance between reactants, taken as the sum of the reaction partner radii. The preexponential factor is given by

$$\tau_s = 4\tau_L \sqrt{\frac{\pi k_B T}{\lambda_s(r)}} \tag{7}$$

where the solvent relaxation time, τ_L, was taken from reference 55 as 260 fs. This corresponds to the average solvation time of acetonitrile. No satisfactory fit could be achieved with the entire set of F/Q pairs when using either the fast, i.e. 89 fs, or the slow, i.e. 630 fs, component of solvation.

The solvent reorganization energy is given by

$$\lambda_s(r) = \frac{e^2}{4\pi\varepsilon_\sigma}\left(\frac{1}{n^2} - \frac{1}{\varepsilon}\right)\left(2 - \frac{\sigma}{r}\right) \tag{8}$$

and the driving force for the photoinduced electron transfer, $\Delta G(r)$, is estimated from the reduction potentials of the donor and acceptor, $E(D^+/D)$ and $E(A/A^-)$, and the energy of the excited reactant, E_{00}, using the Weller equation[7] (Table 1)

$$\Delta G(r) = E(D^+/D) - E(A/A^-) - E_{00} - \frac{e^2}{4\pi\varepsilon_0\varepsilon r} \tag{9}$$

The contact radii, σ, were calculated from the van der Waals molecular volumes (Table 2), the value of ω was taken as 1500 cm^{-1}, and the solvent dielectric constant and refractive index were taken as ε = 36 and n = 1.344.[56] All the other quantities in eqs 4 to 9 were then calculated with these values. The distance dependences of the main quantities are shown in Figure S3, SI. The convolution of the Gaussian instrument response function with eq 1 and eq 2 were compared to the femtosecond emission decays at 0.15 M and to the $\kappa(c)$ dependences, respectively. Good fits to the data were found for several V/L pairs, as these quantities are not independent. Therefore, the best sets of parameters were determined by elaborating two-dimensional maps of the goodness of fit for different values of V, L, and λ_{qm} as discussed in detail in the SI. This procedure also allowed the error on k_0 to be estimated.

dx.doi.org/10.1021/ja4118279 | J. Am. Chem. Soc. 2014, 136, 2026−2032

Table 2. Electron Transfer Parameters Calculated or Obtained from the Data Analysis

F/Q	$-\Delta G$ (eV)	σ (Å)	$k_0 \cdot 10^{-11}$ (M^{-1} s^{-1})	$\kappa_0 \cdot 10^{-11}$ (M^{-1} s^{-1})
DCA/DMB	0.63	7.25	2.9 ± 0.3	0.18
DCA/TMB	0.85	7.07	4.5 ± 1.6	0.18
TCA/TCNE	0.96	6.90	8.9 ± 2.0	0.17
Pe/TMP	1.05	7.24	40.0 ± 7.3	0.26
TrCA/TMB	1.09	7.07	19.5 ± 1.6	0.19
DCA/DMA	1.19	6.87	30.2 ± 3.5	0.24
TCA/TMB	1.35	7.27	33.2 ± 8.0	0.20
TrCA/DMA	1.43	6.97	41.6 ± 13.4	0.24
TCA/DMA	1.69	7.06	39.5 ± 5.0	0.25
CNPe/TCNE	1.74	6.94	28.4 ± 6.3	0.26
DCA/TMP	1.87	7.19	30.0 ± 4.1	0.25
TrCA/TMP	2.11	7.19	31.0 ± 4.7	0.25
Pe/TCNE	2.13	6.85	4.0 ± 1.3	0.25
TCA/TMP	2.37	7.39	21.6 ± 4.5	0.24

Figure 5 shows the excellent agreement between the best fits and the experimental data for TrCA/DMA. Similar good fits were obtained for all 14 F/Q pairs as shown in Figure S5, SI.

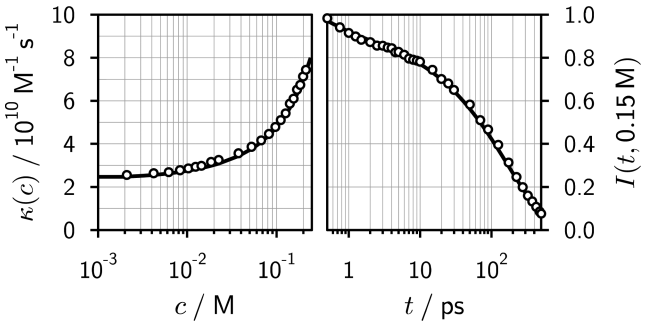

Figure 5. Best fit of the model to the experimental steady-state (left) and femtosecond time-resolved (c = 0.15 M, right) data obtained with TrCA/DMA. Only every ten experimental points of the fluorescence decay are shown to allow better comparison.

Once all the parameters associated with the ET reaction and the diffusion are known, the intrinsic CS rate constant, k_0 (Table 2), were evaluated using the following definition:[41]

$$k_0 = 4\pi \int_{\sigma}^{\infty} w(r) n(r, t = 0) r^2 \mathrm{d}r \qquad (10)$$

where $n(r,t = 0)$ is the radial pair distribution function of the F/Q pair at time zero (cf. SI). The Stern−Volmer quenching constants in the zero quencher concentration limit, κ_0, which is the quantity usually displayed in Rehm−Weller type plots,[8,44,57−61] have also been determined (Table 2).

The resulting intrinsic bimolecular photoinduced CS rate constants, k_0, together with κ_0 are represented as a function of the driving force in Figure 6a. Other κ_0 values taken from references 8, 26, and 44 are also shown for comparison.

The low concentration Stern−Volmer rate constants, κ_0, obtained here are in perfect agreement with previously published values for identical or similar F/Q pairs.[8,26,44] In particular, a diffusional "plateau" at about 2×10^{10} M^{-1} s^{-1}, starting at about 0.15 eV and extending over the entire driving-force range covered is observed. In other words, if one considers the very same experimental observables as in the

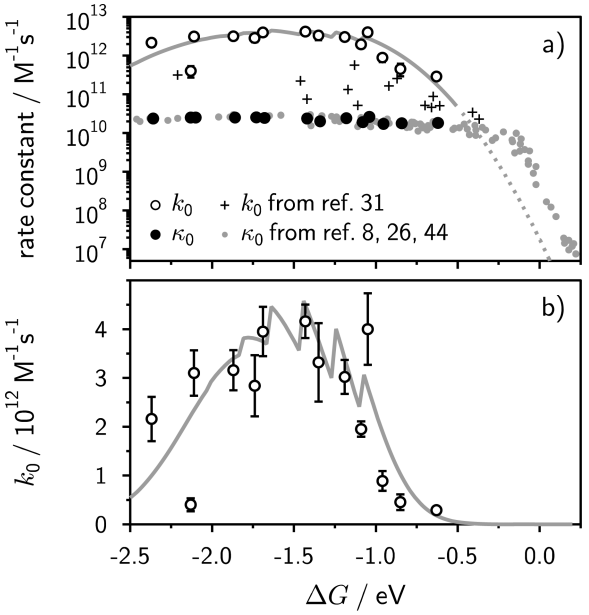

Figure 6. Driving-force dependence of the intrinsic bimolecular CS rate constant (open circles) and of the steady-state quenching rate constant (black circles) and comparison with literature data.[8,26,31,44] The solid line is a simulation calculated using eqs 10 and 4 with σ = 7 Å, V = 72 cm^{-1}, L = 1.29 Å, and λ_{qm} = 0.32 eV.

previous studies, the same absence of an inverted region is found for bimolecular photoinduced CS.

The intrinsic CS rate constants, k_0, are typically 2 orders of magnitude larger than the diffusion-limited rates, κ_0. However, contrary to κ_0, they exhibit a weak driving-force dependence, which can be better appreciated on a linear scale (Figure 6b). The CS rate constant increases by a factor ∼20 when increasing the driving force from 0.6 to 1.6 eV and then shows a 2-fold decrease between 1.6 and 2.4 eV. Thus, the three regions predicted by Marcus ET theory, namely the normal, the barrierless, and the inverted regions can be recognized, although the latter one is very attenuated. Such a bell-shaped behavior was already anticipated from the initial decay of the fluorescence intensity and the static quenching rate at high concentrations by mere inspection. It is thus not due to a bias introduced in the data analysis by the use of the Marcus expression to account for the reaction rate. This is also confirmed by the absence of a trend of the adjustable parameters, V and L, with ΔG (Table S3, SI) that would appear if the driving-force dependence observed here were due to such bias. In fact, the free-energy dependence of k_0 calculated with eq 10 using a single set of V and L nicely reproduces the observed trend (Figure 6). The seesawing features come from the ET model used here and do not necessarily have a physical meaning.[52]

The decrease of the intrinsic rate constant with driving force above ∼1.5 eV points to a very attenuated MIR for bimolecular photoinduced CS, much less pronounced than those observed for other ET processes, as e.g. bimolecular charge recombination or intramolecular charge separation and recombination.[11−14,17] Whereas the CS rate constant decreases here by a factor 2 when increasing the driving force by 0.5 eV in the inverted region, diminutions by 2 orders of magnitude were found for charge recombination.[39] Despite this, the whole driving-force dependence of k_0, including the very shallow inversion can still be satisfyingly reproduced by using Marcus

dx.doi.org/10.1021/ja4118279 | J. Am. Chem. Soc. 2014, 136, 2026−2032

theory. This requires a relatively large electronic coupling element, V, that would give unrealistically large rate constants, if the finite dielectric response of the solvent were not taken into account and if the low coupling limit of eq 4 were used. Therefore, whereas the diffusion limit leads to a leveling off of the κ_0 values, the solvent response results in a similar effect for k_0. Interestingly, essentially the same free energy dependence is obtained if CS is assumed to take place at contact distance only, i.e. if r in eqs 5−9 is kept constant and equal to σ. However, the distance dependence is essential for a correct description of the time-resolved experiments.

Despite the agreement between the ET model and the experiment, one of the differences between CS and charge recombination, where deep inversion is observed, is the existence of excited product states of low energy in the former case. Indeed, the radical ions of most organic molecules have, apart from a few exceptions like $TCNE^{\cdot -}$, low lying electronic excited state, i.e. well below 2 eV, that can be populated when the CS driving force to the ionic product in the ground state is large.[8,21,62,63] Unambiguous evidence of such CS to an excited ionic product was recently reported for the Pe/TCNE pair.[22] The k_0 value found here for this pair is that showing the strongest inversion. However, contrary to the other F/Q pairs, only excited states of $F^{\cdot +}$ can be populated. In the other pairs, such as e.g. TCA/TMP, both radical anion and cation have sufficiently low electronic excited states.[64] The existence of these additional pathways leads to an increase of the CS rate constants, hence to an additional attenuation of the MIR.

Considering the above results, the persisting lack of observations of the Marcus inverted region for bimolecular photoinduced CS using only steady-state and/or nanosecond time-resolved emission spectroscopy is not at all bewildering. Figure 6 shows that the CS remains significantly faster than diffusion in liquid solution up to a driving force of at least 2.5 eV.

The intrinsic CS rate constants reported by Mataga and co-workers[31] (+'s in Figure 6a) and obtained using a similar combination of time-resolved measurements and analysis with a model for diffusion-assisted reaction are substantially smaller and more scattered than those obtained in this work. These differences most probably originate from the response time of their experiment, which was more than 2 orders of magnitude larger than that of the fluorescence up-conversion setup used here. As steady-state quenching experiments were not used to check the consistency of the time-resolved data analysis, ultrafast quenching components, beyond the resolution of their experiment, have probably been missed.

Around $\Delta G = 0$, a horizontal shift of approximately 0.2 eV between our extrapolated simulation and the original experimental Rehm and Weller results can be seen. This difference could originate from too simplistic an estimation of the CS driving force when using eq 9. For example, the adequacy of the Coulombic term in eq 9 to account for the electrostatic interaction between two ions in contact has been questioned.[65] Furthermore, exciplexes with partial charge transfer character have been shown to be the dominant product of weakly exergonic ET quenching.[61,66−69] In such cases, the effective driving force is not properly accounted for by eq 9 that assumes full charge transfer.

CONCLUSIONS

Contrary to previous investigations of the driving-force dependence of bimolecular photoinduced charge separation processes, we have focused our attention on the static and transient stages of the fluorescence quenching using a combination of steady-state and femtosecond time-resolved emission measurements. By analyzing both sets of data with differential encounter theory, we have been able to obtain the intrinsic rate constants of bimolecular photoinduced charge separation in acetonitrile. A weak bell-shape dependence of the quenching rate, which can already be anticipated by direct inspection of the experimental data, is found. The charge separation rate constant increases up to a driving force of about 1.5 eV and exhibits a slight decrease at higher driving forces. Charge separation remains faster than diffusion by almost 2 orders of magnitude over the whole ΔG range investigated. These large rate constants and weak decrease explain why the Marcus inverted region could never be observed when looking at the slower stages of the quenching, using nanosecond time-resolved fluorescence and/or steady-state quenching experiments at low concentration. This solves the long-lasting paradox related to the Rehm−Weller experiment. The driving-force dependence found here for bimolecular photoinduced charge separation is much less pronounced than those reported for other electron transfer processes. It can be explained by the opening of new charge separation channels at high exergonicity leading to the formation of excited ion products, as recently observed.[22] Even neglecting these additional pathways, the observed driving-force dependence can be accounted for in terms of Marcus theory, taking the solvent dielectric response into account.

ASSOCIATED CONTENT

Supporting Information

Detailed description of the experimental procedures. Equilibrium constants for the ground-state charge transfer complexes. Characterization of the solvent/quencher mixtures. Detailed outline of the diffusion-reaction equation approach used. Discussion of the alternative fitting attempts. Concentration-normalized time-profiles, femtosecond fluorescence decays and concentration dependence of the steady-state quenching rates of all 14 systems studied. Detailed procedure of the error estimation of the electron transfer parameters. This material is available free of charge via the Internet at http://pubs.acs.org.

AUTHOR INFORMATION

Corresponding Author

eric.vauthey@unige.ch

Notes

The authors declare no competing financial interest.

ACKNOWLEDGMENTS

The authors thank Prof. Anatoly I. Ivanov (Volgograd State University) and Dr. Bernhard Lang (University of Geneva) for their helpful comments. This work was supported by the Fonds National Suisse de la Recherche Scientifique through Project No. 200020-147098 and the NCCR MUST, and by the University of Geneva. Financial support from European Union 7.FP under grant REGPOT-CT-2011-285949-NOBLESSE is gratefully acknowledged.

REFERENCES

(1) Marcus, R. A. *J. Chem. Phys.* **1956**, *24*, 966.
(2) Evans, M. G.; Polanyi, M. *Trans. Faraday Soc.* **1935**, *31*, 875.
(3) Bell, R. P. *Proc. R. Soc. London, Ser. A* **1936**, *154*, 414.

(4) Carey, F. A.; Sundberg, R. J. *Advanced Organic Chemistry: Part A: Structure and Mechanisms*; Springer: New York, 2007.
(5) Dulz, G.; Sutin, N. *Inorg. Chem.* **1963**, *2*, 917.
(6) Sutin, N. *Acc. Chem. Res.* **1968**, *1*, 225.
(7) Rehm, D.; Weller, A. *Ber. Bunsenges. Phys. Chem.* **1969**, *73*, 834.
(8) Rehm, D.; Weller, A. *Isr. J. Chem.* **1970**, *8*, 259.
(9) Miller, J. R.; Calcaterra, L. T.; Closs, G. L. *J. Am. Chem. Soc.* **1984**, *106*, 3047.
(10) Closs, G. L.; Miller, J. R. *Science* **1988**, *240*, 440.
(11) Wasielewski, M. R.; Niemczyk, M. P.; Svec, W. A.; Pewitt, E. B. *J. Am. Chem. Soc.* **1985**, *107*, 1080.
(12) Gould, I. R.; Ege, D.; Mattes, S. L.; Farid, S. *J. Am. Chem. Soc.* **1987**, *109*, 3794.
(13) Mataga, N.; Asahi, T.; Kanda, Y.; Okada, T.; Kakitani, T. *Chem. Phys.* **1988**, *127*, 249.
(14) Vauthey, E.; Suppan, P.; Haselbach, E. *Helv. Chim. Acta* **1988**, *71*, 93.
(15) Guldi, D. M.; Asmus, K. D. *J. Am. Chem. Soc.* **1997**, *119*, 5744.
(16) Fukuzumi, S.; Ohkubo, K.; Imahori, H.; Guldi, D. M. *Chem.—Eur. J.* **2003**, *9*, 1585.
(17) Mataga, N.; Chosrowjan, H.; Shibata, Y.; Yoshida, N.; Osuka, A.; Kikuzawa, T.; Okada, T. *J. Am. Chem. Soc.* **2001**, *123*, 12422.
(18) Smitha, M. A.; Prasad, E.; Gopidas, K. R. *J. Am. Chem. Soc.* **2001**, *123*, 1159.
(19) Rosspeintner, A.; Koch, M.; Angulo, G.; Vauthey, E. *J. Am. Chem. Soc.* **2012**, *134*, 11396.
(20) Turro, N. J.; Ramamurthy, V.; Scaiano, J. C. *Modern Molecular Photochemistry of Organic Molecules*; University Science Books: Mill Valley, CA, 2010.
(21) Siders, P.; Marcus, R. A. *J. Am. Chem. Soc.* **1981**, *103*, 748.
(22) Koch, M.; Rosspeintner, A.; Adamczyk, K.; Lang, B.; Dreyer, J.; Nibbering, E. T. J.; Vauthey, E. *J. Am. Chem. Soc.* **2013**, *135*, 9843.
(23) Yoshimori, A.; Kakitani, T.; Enomoto, Y.; Mataga, N. *J. Phys. Chem.* **1989**, *93*, 8316.
(24) Tachiya, M.; Murata, S. *J. Phys. Chem.* **1992**, *96*, 8441.
(25) Burshtein, A. I.; Ivanov, A. I. *Phys. Chem. Chem. Phys.* **2007**, *9*, 396.
(26) Rosspeintner, A.; Kattnig, D. R.; Angulo, G.; Landgraf, S.; Grampp, G. *Chem.—Eur. J.* **2008**, *14*, 6213.
(27) Brunschwig, B. S.; Ehrenson, S.; Sutin, N. *J. Am. Chem. Soc.* **1984**, *106*, 6858.
(28) Murata, S.; Matsuzaki, S. Y.; Tachiya, M. *J. Phys. Chem.* **1995**, *99*, 5354.
(29) Eads, D. D.; Dismer, B. G.; Fleming, G. R. *J. Chem. Phys.* **1990**, *93*, 1136.
(30) Weidemaier, K.; Tavernier, H. L.; Swallen, S. F.; Fayer, M. D. *J. Phys. Chem. A* **1997**, *101*, 1887.
(31) Nishikawa, S.; Asahi, T.; Okada, T.; Mataga, N.; Kakitani, T. *Chem. Phys. Lett.* **1991**, *185*, 237.
(32) Angel, S. A.; Peters, K. S. *J. Phys. Chem.* **1991**, *95*, 3606.
(33) Grampp, G.; Kelterer, A.-M.; Landgraf, S.; Sacher, M.; Niethammer, D.; Telo, J. P.; Dias, R. M. B.; Vieira, A. J. S. C. *Monatsh. Chem.* **2005**, *136*, 519.
(34) Mattes, S. L.; Farid, S. *J. Am. Chem. Soc.* **1982**, *104*, 1454.
(35) Kikuchi, K.; Takahashi, Y.; Hoshi, M.; Niwa, T.; Katagiri, T.; Miyashi, T. *J. Phys. Chem.* **1991**, *95*, 2378.
(36) Gould, I. R.; Moser, J. E.; Armitage, B.; Farid, S. *J. Am. Chem. Soc.* **1989**, *111*, 1917.
(37) Kikuchi, K.; Niwa, T.; Takahashi, Y.; Ikeda, H.; Miyashi, T. *J. Phys. Chem.* **1993**, *97*, 5070.
(38) Vauthey, E.; Högemann, C.; Allonas, X. *J. Phys. Chem. A* **1998**, *102*, 7362.
(39) Vauthey, E. *J. Phys. Chem. A* **2001**, *105*, 340.
(40) Rosspeintner, A.; Angulo, G.; Vauthey, E. *J. Phys. Chem. A* **2012**, *116*, 9473.
(41) Burshtein, A. I. *Adv. Chem. Phys.* **2004**, *129*, 105.
(42) Koch, M.; Rosspeintner, A.; Angulo, G.; Vauthey, E. *J. Am. Chem. Soc.* **2012**, *134*, 3729.
(43) Valeur, B. *Molecular Fluorescence. Principles and Applications*, Wiley-VCH: Weinheim, 2001.
(44) Niwa, T.; Kikuchi, K.; Matsusita, N.; Hayashi, M.; Katagiri, T.; Takahashi, Y.; Miyashi, T. *J. Phys. Chem.* **1993**, *97*, 11960.
(45) Rice, S. A. *Diffusion Limited Reactions*; Comprehensive Chemical Kinetics, Vol. *25*; Elsevier: New York, 1985.
(46) Wilemski, G.; Fixman, M. *J. Chem. Phys.* **1973**, *58*, 4009.
(47) Tachiya, M. *Radiat. Phys. Chem.* **1983**, *21*, 167.
(48) Dorfman, R. C.; Fayer, M. D. *J. Chem. Phys.* **1992**, *96*, 7410.
(49) Sailer, C. F.; Thallmair, S.; Fingerhut, B. P.; Nolte, C.; Ammer, J.; Mayr, H.; Pugliesi, I.; de Vivie-Riedle, R.; Riedle, E. *ChemPhysChem* **2013**, *14*, 1423.
(50) Rosspeintner, A.; Kattnig, D. R.; Angulo, G.; Landgraf, S.; Grampp, G.; Cuetos, A. *Chem. - Eur. J.* **2007**, *13*, 6474.
(51) Angulo, G.; Kattnig, D. R.; Rosspeintner, A.; Grampp, G.; Vauthey, E. *Chem.—Eur. J.* **2010**, *16*, 2291.
(52) Gould, I. R.; Young, R. H.; Moody, R. E.; Farid, S. *J. Phys. Chem.* **1991**, *95*, 2068.
(53) Newton, N. D.; Sutin, N. *Annu. Rev. Phys. Chem.* **1984**, *35*, 437.
(54) Wynne, K.; Hochstrasser, R. M. *Adv. Chem. Phys.* **1999**, *107*, 263.
(55) Horng, M. L.; Gardecki, J. A.; Papazyan, A.; Maroncelli, M. *J. Phys. Chem.* **1995**, *99*, 17311.
(56) Riddick, J. A.; Bunger, W. B. *Organic Solvents*; John Wiley: New York, 1970.
(57) Inada, T. N.; Miyazawa, C. S.; Kikuchi, K.; Yamauchi, M.; Nagata, T.; Takahashi, Y.; Ikeda, H.; Miyashi, T. *J. Am. Chem. Soc.* **1999**, *121*, 7211.
(58) Del Negro, A. S.; Seliskar, C. J.; Heineman, W. R.; Hightower, S. E.; Bryan, S. A.; Sullivan, B. P. *J. Am. Chem. Soc.* **2006**, *128*, 16494.
(59) Farid, S.; Dinnocenzo, J. P.; Merkel, P. B.; Young, R. H.; Shukla, D.; Guirado, G. *J. Am. Chem. Soc.* **2011**, *133*, 11580.
(60) Matsuda, N.; Kakitani, T.; Denda, T.; Mataga, N. *Chem. Phys.* **1995**, *190*, 83.
(61) Gould, I. R.; Young, R. H.; Mueller, L. J.; Farid, S. *J. Am. Chem. Soc.* **1994**, *116*, 8176.
(62) Pagès, S.; Lang, B.; Vauthey, E. *J. Phys. Chem. A* **2004**, *108*, 549.
(63) Gladkikh, V.; Burshtein, A. I.; Angulo, G.; Pagès, S.; Lang, B.; Vauthey, E. *J. Phys. Chem. A* **2004**, *108*, 6667.
(64) Shida, T. *Electronic Absorption Spectra of Radical Ions*; Physical Sciences Data, Vol. *34*; Elsevier: Amsterdam, 1988.
(65) Suppan, P. *J. Chem. Soc., Faraday Trans. I* **1986**, *82*, 509.
(66) Kikuchi, K.; Niwa, T.; Takahashi, Y.; Ikeda, H.; Miyashi, T.; Hoshi, M. *Chem. Phys. Lett.* **1990**, *173*, 421.
(67) Nicolet, O.; Vauthey, E. *J. Phys. Chem. A* **2003**, *107*, 5894.
(68) Farid, S.; Dinnocenzo, J. P.; Merkel, P. B.; Young, R. H.; Shukla, D. *J. Am. Chem. Soc.* **2011**, *133*, 4791.
(69) Richert, S.; Rosspeintner, A.; Landgraf, S.; Grampp, G.; Vauthey, E.; Kattnig, D. R. *J. Am. Chem. Soc.* **2013**, *135*, 15144.